We are IntechOpen, the world's leading publisher of Open Access books Built by scientists, for scientists

7,000
Open access books available

186,000
International authors and editors

200M
Downloads

154
Countries delivered to

Our authors are among the

TOP 1%
most cited scientists

12.2%
Contributors from top 500 universities

CLARIVATE ANALYTICS
BOOK CITATION INDEX
INDEXED

WEB OF SCIENCE™

Selection of our books indexed in the Book Citation Index
in Web of Science™ Core Collection (BKCI)

Interested in publishing with us?
Contact book.department@intechopen.com

Numbers displayed above are based on latest data collected.
For more information visit www.intechopen.com

8

Practical Control Method for Two-Mass Rotary Point-To-Point Positioning Systems

Fitri Yakub, Rini Akmeliawati and Aminudin Abu
Malaysia-Japan International Institute of Technology (MJIIT),
Universiti Teknologi Malaysia International Campus (UTM IC)
Malaysia

1. Introduction

Motion control systems play an important role in industrial engineering applications such as advanced manufacturing systems, semiconductor manufacturing system, computer numerical control (CNC) machining and robot systems. In general, positioning system can be classified into two types, namely point-to-point (PTP) positioning systems and continuous path (CP) control system (Crowder R.M, 1998). PTP positioning systems, either of one-mass or multi-mass systems, is used to move an object from one point to another point either in angular or linear position. For example, in application with one-mass system, such as CNC machines, PTP positioning is used to accurately locate the spindle at one or more specific locations to perform operations, such as drilling, reaming, boring, tapping, and punching. In multi-mass systems application, such as in spot-welding robot, which has a long arm for linear system or long shaft in rotary system, PTP positioning is used to locate the manipulator from one location to another.

PTP positioning system requires high accuracy with a high speed, fast response with no or small overshoot and to be robust to parameter variations and uncertainties. Therefore, the most important requirements in PTP positioning systems are the final accuracy and transition time whereas the transient path is considered as the second important. However, it is not easy to achieve high precision performances because of non-linearities and uncertainties exist in the motion control systems. One significant nonlinearity is friction that causes steady state error and/or limit cycles near the reference position (Armstrong et al., 1994). Another source of nonlinearity in motion control system is saturation of the actuator and/or electronic power amplifier. Saturation causes slow motion and may effect the stability of the performances (Slotine & Li, 1991). In PTP applications, the system performance is expected to be the same or as close as its performance when the system is in normal condition. Thus, robustness is also an important requirement in order to maintain the stability of the positioning systems.

In order to satisfy the design requirements, a good controller is required. Many types of controllers have been proposed and evaluated for positioning systems. The use of proportional-integral-derivative (PID) controllers are the most popular controller used in industrial control systems including motion control systems due to their simplicity and also

satisfactory performances (Yonezawa et al., 1990). However, it is difficult to achieve a fast response with no or small overshoot simultaneously.

In practical applications, an engineer does not need deep knowledge or be an expert in control systems theory while designing controllers. Thus, easiness of controller design process, simplicity of the controller structure and no requirement of exact object model and its parameters are very important and preferable in real applications. To achieve these, nominal characteristic trajectory following (NCTF) controller for one-mass rotary systems had been proposed as a practical controller for PTP positioning systems in (Wahyudi, 2002). The controller design procedure is simple and easily implemented since it is only based on a simple open-loop experiment. In addition, an exact object model and its parameters does not required while designing the controller. Thus, this controller is easy to design, adjustable and understands.

The NCTF controller had been proposed as a practical controller for PTP positioning systems. However, the NCTF controller is designed based on one-mass rotary positioning systems. Positioning system was considered as a one-mass system when a rigid coupling with high stiffness is used. The existing NCTF controller does not work for two-mass rotary system because of the vibration happened due to mechanical resonance of the plant such as flexible coupling or a long shaft with low stiffness are used. This vibration gives the unstable performance response of the plant. Therefore, enhancement and improvement design of NCT and a compensator are required to make the NCTF controller suitable for two-mass rotary positioning systems, which have long shaft between the actuator and load. This chapter is an attempt to address the problem of NCTF for two-mass system or multi-mass systems.

2. Basic concept of NCTF controller

The structure of the NCTF control system is shown in Figure 1 (Mohd Fitri Mohd Yakub et al., 2010) consists of:

a. A nominal characteristic trajectory (NCT) that is constructed based on measured θ_l, and $\dot{\theta}_l$, which were obtained by a simple open-loop experiment. Thus, the NCT provides information of characteristics of the system, which can be used to design a compensator.
b. A compensator which is used to force the object motion to reach the NCT as fast as possible, control the object motion to follow the NCT, and end it at the origin of the phase-plane $\left(e = 0, \dot{e} = 0 \right)$ as shown in Figure 2.

Therefore, the controller is called as the NCTF controller.

As shown in Figure 1, the controller output is signal u. This signal is used to drive the object. The input to the controller are error, e, and object motion, $\dot{\theta}_l$. In principle, the controller compares the object motion input, $\dot{\theta}_l$ with the error-rate, $\dot{e}$, provided by predetermined NCT, at certain error. The difference between the actual error-rate of the object and that of the NCT is denoted as signal u_p, which is the output of the NCT. If the object motion perfectly follows the NCT, the value of signal u_p is zero. Thus, no action is performed by the

compensator. When the signal u_p is not zero, the compensator is used to drive the value of signal u_p to zero.
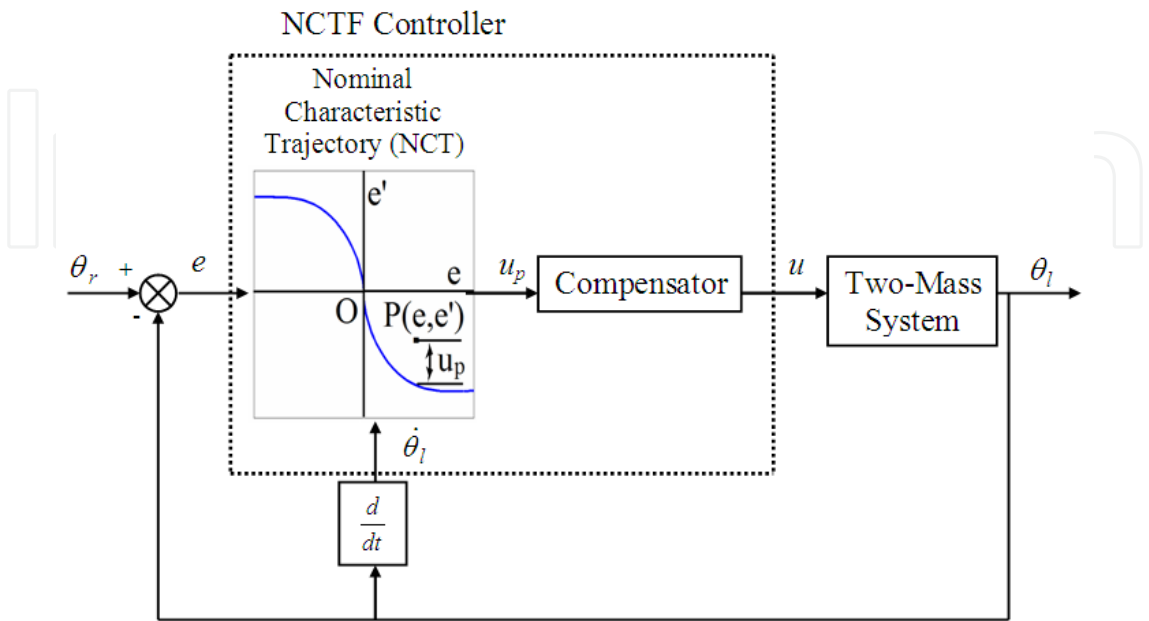

Fig. 1. Structure of NCTF control system

In Figure 2, the object motion is divided into two phases, the reaching phase and the following phase. During the reaching phase, the compensator forces the object motion to reach the NCT as fast as possible. Then, in the following phase, the compensator controls the object motion to follow the NCT and end at the origin. The object motion stops at the origin, which represents the end of the positioning motion. Thus, the NCT governs the positioning response performance.
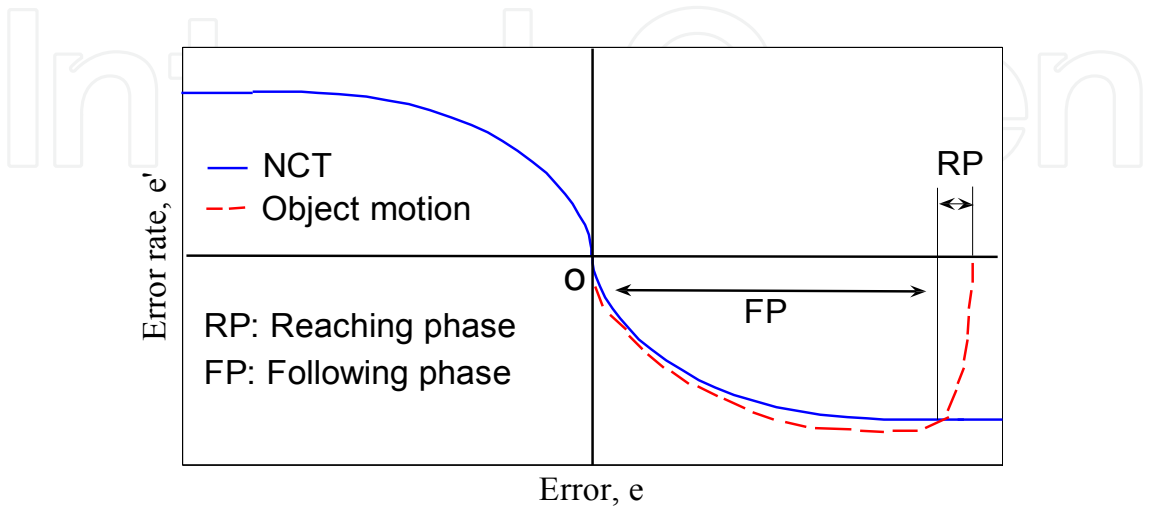
Fig. 2. NCT and object motion

The electric motor is assumed as the actuator in this discussion. To drive the object to reach the NCT, the actuator needs to reach its maximum velocity. The characteristic of the actuator when it stops from its maximum velocity influences the final accuracy of the PTP positioning operation. Thus, this characteristic is required to design the controller. In order to obtain the required characteristics, conducting a simple open-loop experiment is a simple and practical way.

In summary, the structure of the NCTF control system for PTP positioning systems shown in Figure 1 only works under the following two conditions (Wahyudi et al., 2003):

i.   A DC or an AC servomotor is used as an actuator of the object.

ii.   The reference input, θ_r is constant and $\dot{\theta}_r = 0$.

3. Practical controller design

The NCTF controller consists of NCT, which is constructed based on a simple open-loop experiment of the object, and PI compensator, which is designed based on the obtained NCT. Therefore, the design of NCTF controller can be described by the following steps:

i.   The object is driven with an open loop stepwise input and its load displacement and load velocity responses are measured.

ii.   Construct the NCT by using the object responses obtained during the deceleration process. Since the NCT is constructed based on the actual responses of the object, it contains nonlinear characteristics such as friction and saturation. The NCTF controller is expected to avoid impertinent behaviour by using the NCT.

iii. Design the compensator based on the open-loop responses and the NCT information. In order to consider the real characteristic of the mechanism in designing compensator, a practical stability analysis is determined.

The NCT includes information of the actual object parameters. Therefore, the compensator can be designed by using only the NCT information. Due to the fact that the NCT and the compensator are constructed from a simple open-loop experiment of the object, the exact model including the friction characteristic and the conscious identification task of the object parameters are not required to design the NCTF controller. The controller adjustment is easy and the aims of its control parameters are simple and clear.

3.1 NCT constructions

As mentioned earlier, in order to construct the NCT, a simple open-loop experiment has to be conducted. In the experiment, an actuator of the object is driven with a stepwise input and, load displacement and load velocity responses of the object are measured. Figure 3 shows the stepwise input, load velocity and load displacement responses of the object. In this case, the object vibrates due to its mechanical resonance. In order to eliminate the influence of the vibration on the NCT, the object response must be averaged.

In Figure 4(a), moving average filter is used to get the averaged response because of its simplicity (Oppenheim & Schafer, 1999). The moving average filter operates by averaging a number of points from the object response to produces each point in the averaged response. Mathematically, it can be expressed as follows:

$$\theta_{av}(i) = \frac{1}{M} \sum_{j=-(M-1)/2}^{(M-1)/2} \theta(i+j) \qquad (1)$$

$$\dot{\theta}_{av}(i) = \frac{1}{M} \sum_{j=-(M-1)/2}^{(M-1)/2} \dot{\theta}(i+j) \qquad (2)$$

where θ represents the object displacement in rad, θ' the object velocity in rad/s, θ_{av} the averaged object displacement, θ'_{av} the averaged object velocity and M is the number of data points of the object responses used in the averaging process. The averaged velocity and displacement responses are used to determine the NCT. Since the main problem of the PTP motion control is to stop an object at a certain position, a deceleration process (curve in area A of Figure 4) is used. The phase plane of the NCT has a horizontal axis of error, e, and a vertical axis of error-rate, $\dot{e}$, as shown in Figure 4(b). The horizontal axis shows the error from the desired position. Therefore, the values are taken from the displacement data of the open-loop responses. The error is the displacement data when it started entering deceleration process subtracted by the maximum displacement. The error-rate is the velocity data within the deceleration process. In Figure 4(a), h is the maximum velocity which depends on the input step height, and is gradually decreasing until zero. Thus, the pair data of error and error-rate construct the NCT, i.e. the phase-plane diagram of e and $\dot{e}$.
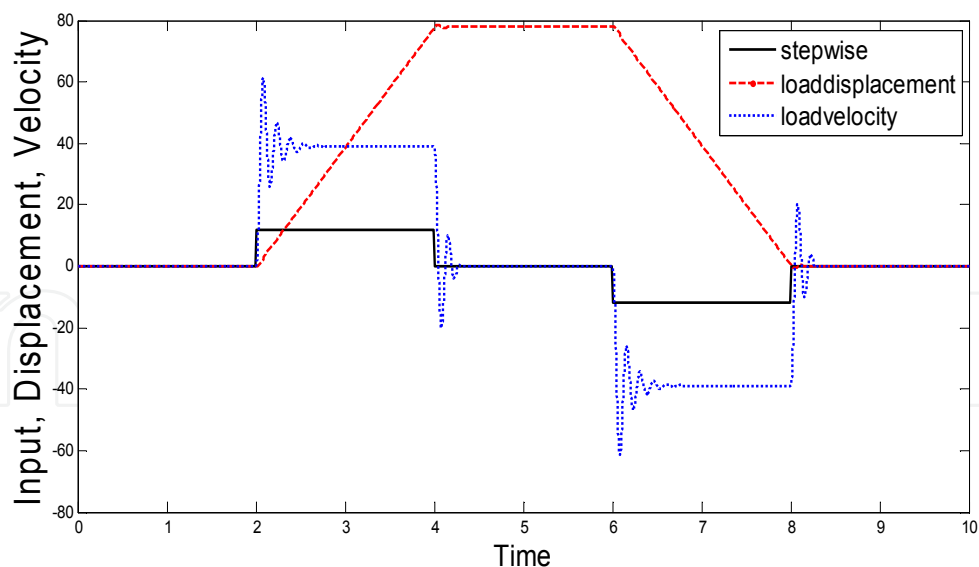

Fig. 3. Input and actual object response

From the response, the maximum velocity of the actuator is obtained. Important characteristics of the actuator can be identified from the data within the deceleration range. In the deceleration process, the actuator moves freely from its maximum velocity until it stops.

In the deceleration process, non-linearity characteristics such as friction and saturation of the object have taken its effect. Therefore, the data can be translated into the form that represents the system characteristics including friction and saturation. From the curve in area *A* and *h* in Figure 4(a), the NCT in Figure 4(b) is determined.
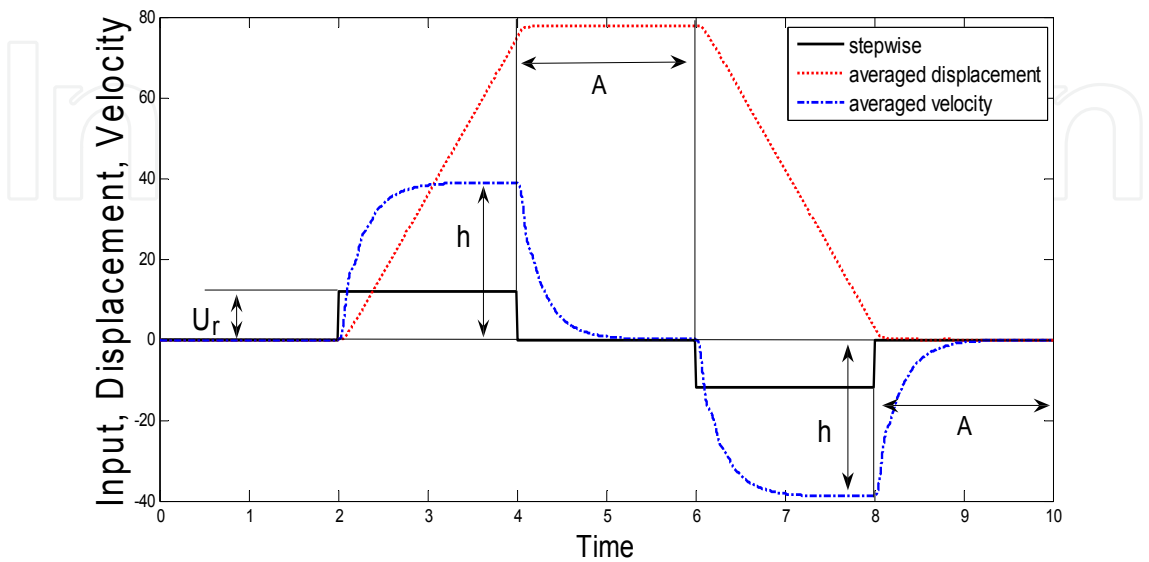
a) Input and averaged object response
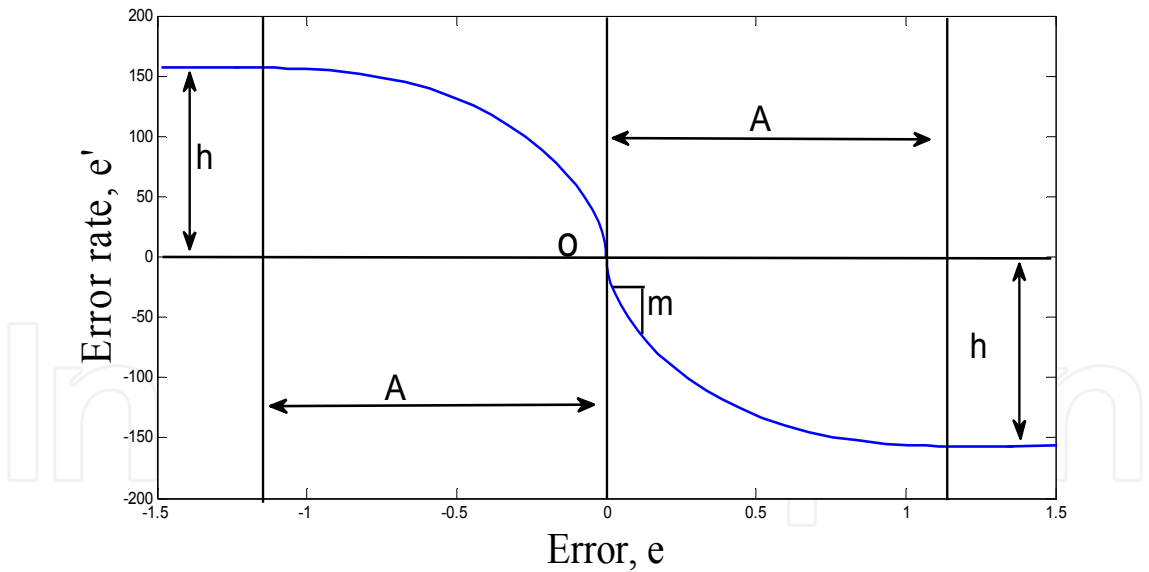
b) Nominal characteristic trajectory

Fig. 4. Construction of the NCT.

There are two important parameters in the NCT as shown in Figure 4(b), the maximum error indicated by *h* and the inclination of the NCT near the origin indicated by *m*. This parameter is related to the dynamics of the object. Therefore, these parameters can be used to design the compensator.

3.2 Simplified object parameters

An exact modeling, including friction and conscious identification processes, is not required in the NCTF controller design. The compensator is derived from the parameter m and h of the NCT. Since the DC motor is used as the actuator, the simplified object can be presented as a following fourth-order system (Dorf, & Bishop, 2008):

$$G_o(s) = \frac{\theta_l(s)}{U(s)} = K \frac{\alpha_2}{s(s+\alpha_2)} \frac{\omega_f^2}{s^2 + 2\zeta_f \omega_f s + \omega_f^2} \tag{1}$$

where θ_l (s) represents the displacement of the object, $U(s)$, the input to the actuator and K, ζ, a_2 and ω_f are simplified object parameters. The NCT is determined based on the averaged object response which does not include the vibration. So, it can be assumed that the averaged object response is a response to the stepwise inputs of the averaged object model as follows:

$$\frac{\theta_l(s)}{U(s)} = K \frac{\alpha_2}{s(s+\alpha_2)} \tag{2}$$

where $\theta_l(s)$ represents the displacement of the object, $U(s)$ is an input to the actuator, and, K and a_2 are simplified object parameters. This simplified model is reasonable since it is assumed that a DC or AC servomotor is used to drive the positioning systems. The simplified object model of Eq. (2) can be described in the state space representation as follow:

$$\frac{d}{dt} \begin{bmatrix} \theta_l \\ \dot{\theta}_l \end{bmatrix} = \begin{bmatrix} 0 & 1 \\ 0 & -\alpha_2 \end{bmatrix} \begin{bmatrix} \theta_l \\ \dot{\theta}_l \end{bmatrix} + \begin{bmatrix} 0 \\ \alpha_2 K \end{bmatrix} u \tag{3}$$

Characteristic of the positioning systems near the reference position is very important because system stability and positioning accuracy depend on it characteristic. The inclination m of the NCT near the origin is related to the simplified object parameter α_2. The NCT in Figure 4(b) shows,

$$\frac{d\dot{e}}{de} = m \tag{4}$$

The NCT inclination near the origin m is constructed when the input to the object is zero $(u = 0)$. By letting $u = 0$ in Eq. (3),

$$\frac{d\dot{\theta}_l}{d\theta_l} = -\alpha_2 \tag{5}$$

As considering $e = \theta_r - \theta$ and θ_r is constant in the case of PTP positioning systems. Then, Eq. (5) is translated to the following form,

$$\frac{d\dot{e}}{de} = -\alpha_2 \tag{6}$$

Hence, from Eqs. (4) and (6), we obtain,

$$\alpha_2 = -m \tag{7}$$

The value of the maximum error rate h of the NCT is related to the steady-state velocity due to input actuator u_p. Based on the final value theorem, the steady-state velocity is Ku_r. Then,

$$h = -Ku_r \tag{8}$$

Thus, K can be expressed as,

$$K = \frac{h}{u_r} \tag{9}$$

The friction characteristic influences the NCT inclination near the origin m and the maximum error rate of h of the NCT. Therefore, the simplified object model includes the effect of friction when they are determined with Eqs. (8) and (9).

3.3 Compensator design

The following proportional integral (PI) and notch filter (NF) compensator is proposed for two-mass systems:

$$G_c(s) = \frac{(K_p s + K_i)}{s}\left(\frac{K_{dc}(s^2 + 2\zeta_f \omega_f s + \omega_f^2)}{(s^2 + 2\zeta_o \omega_o s + \omega_o^2)}\right) \tag{10}$$

where K_p is the proportional gain, K_i is the integral gain, K_{dc} is the filter gain, ζ_f and ω_f represent zeros of NF, while ζ_o and ω_o represent poles of NF. The PI compensator is adopted for its simplicity to force the object motion to reach the NCT as fast as possible and control the object motion to follow the NCT and stop at the origin.

Figure 5 shows the block diagram of the continuous close-loop NCTF control system with the simplified object near the NCT origin where the NCT is linear and has an inclination $a_2=-m$. The signal u_p near the NCT origin in Figure 5 can be expressed as the following equation:

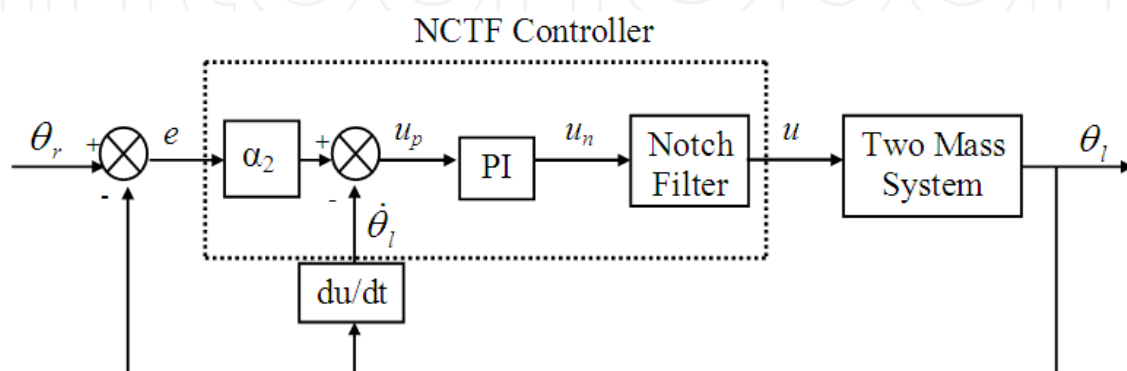$$u_p = \dot{e} + \alpha_2 e = \alpha_2 e - \dot{\theta}_l \tag{11}$$

Fig. 5. Simplified NCTF control system

The PI compensator is designed based on the simplified object parameters, which are also related to the NCT, i.e h and m. Due to its simplicity, the following PI compensator is adopted.

$$G_c(s) = K_p + \frac{K_i}{s} \tag{12}$$

According to the signal u_p given by Eq. (11) and the simplified object model in Eq. (2), the NCTF control system in Figure 1 can be represented by block diagram as shown in Figure 6. Using the PI compensator parameters K_p and K_i, and the simplified object model in Eq. (2), the transfer function near the origin of the closed-loop system for the NCTF controller in Figure 1 is,

$$\frac{\theta_l(s)}{\theta_r(s)} = \frac{\alpha_2}{s+\alpha_2} G(s) \tag{13}$$

where,

$$G(s) = \frac{\alpha_2 KK_p s + \alpha_2 KK_i}{s^2 + \alpha_2 KK_p s + \alpha_2 KK_i} \tag{14}$$

(a)

(b)
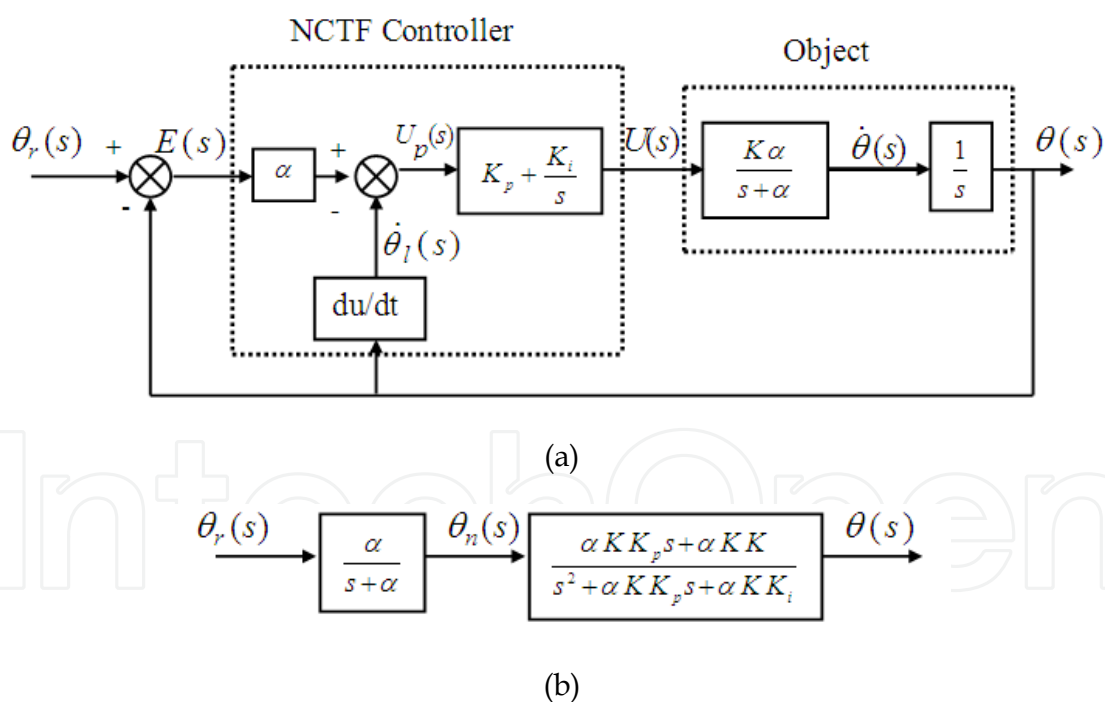
Fig. 6. NCTF control system near the origin: (a) Linearized block diagram, (b) Linearized closed-loop transfer function

$G(s)$ given by Eq. (13) can be rewritten in the following form;

$$G(s) = \frac{2\zeta\omega_n s + \omega_n^2}{s^2 + 2\zeta\omega_n s + \omega_n^2} \tag{15}$$

where,

$$\alpha_2 K K_p = 2\zeta\omega_n \tag{16}$$

$$\alpha_2 K K_i = \omega_n^2 \tag{17}$$

In the case of $G(s) = 1$, Eq. (13) become;

$$\frac{\theta_l(s)}{\theta_r(s)} = \frac{\alpha_2}{s + \alpha_2} \tag{18}$$

In PTP positioning systems, Eq. (18) can be rewritten in time domain as follow:

$$\dot{e} + \alpha_2 e = 0 \tag{19}$$

From Eq. (11), it can be said that Eq. (19) represents the condition for $u_p = 0$. Since u_p indicates the difference between the object motion and the NCT, it can be concluded that the object motion follows the NCT perfectly if $G(s) = 1$. Therefore, the PI compensator parameters should be designed based on ω_n and ζ so that $G(s) = 1$.

The PI compensator parameters, K_p and K_i can be expressed as a function of the natural frequency and the damping ratio as follows:

$$K_p = \frac{2\zeta\omega_n}{\alpha_2 K} = \frac{2\zeta\omega_n u_r}{mh} \tag{20}$$

$$K_i = \frac{\omega_n^2}{\alpha_2 K} = \frac{\omega_n^2 u_r}{mh} \tag{21}$$

A higher ω_n and a larger ζ are preferable in the compensator design. However, while choosing ζ and ω_n, the designer must consider the stability of the control system. In continuous system, a linear stability limit can be calculated independently of the actual mechanism characteristic. However, the stability limit is too limited because of neglected Coulomb friction is known to increase the stability of the system, allowing for the use of higher gains than those predicted by a linear analysis (Townsend WT & Kenneth Salisbury J, 1987).

The higher gains are expected to produce a higher positioning performance. Thus the practical stability limit is necessary for selecting the higher gain in a design procedure. The selection of ω_n and ζ are chosen to have 40% of the values of ζ_{prac}, so that the margin safety of design is 60% (Guilherme Jorge Maeda & Kaiji Sato, 2007). Figure 7 shows the various margin safeties based on practical stability limit, ζ_{prac}. During the design parameter selection, the designer may be tempted to use large values of ω_n and ζ in order to improve the performance. However, excessively large values of ω_n will cause the controller to behave as a pure integral controller, which may lead to instability. Therefore, the choice of ω_n should start with small values and progress to larger one and not the other hand.
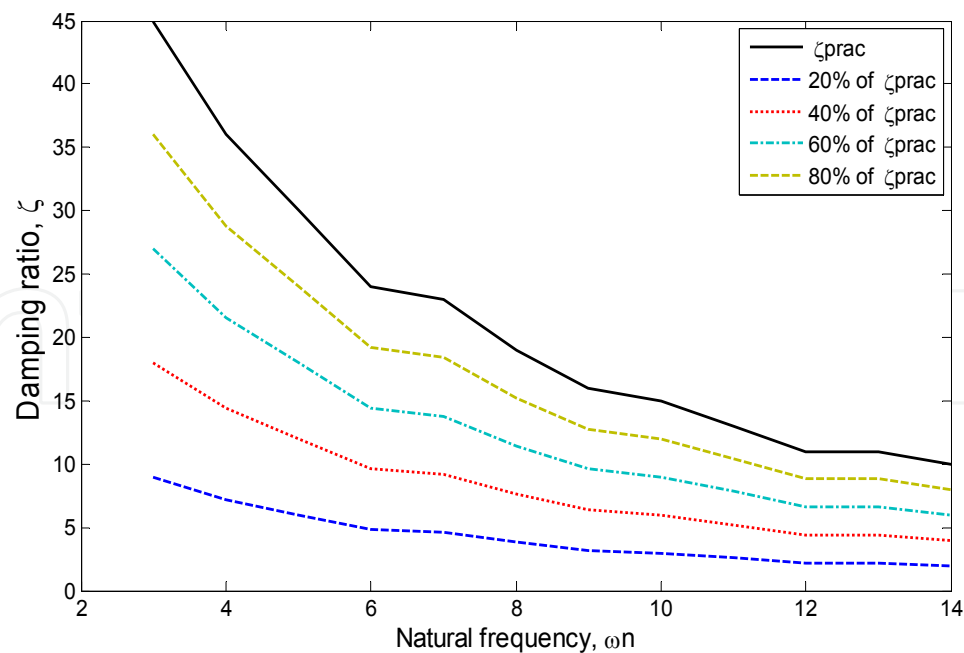
Fig. 7. Practical stability limit respecting a various margin of safety

Figure 8 shows the positioning performance response due to 0.5 deg step input. It is shown that the best performance was in between 60% to 80% margin of safety.

In many systems, the mechanical couplings between the motor, load, and sensor are not perfectly rigid, but instead act like springs. Here, the motor response may overshoot or even oscillate at the resonance frequency resulting in longer settling time. The most effective way to deal with this torsional resonance is by using an anti resonance notch filter.

According to standard frequency analysis, resonance is characterized by a pair of poles in the complex frequency plane. The imaginary component indicates the resonant frequency,
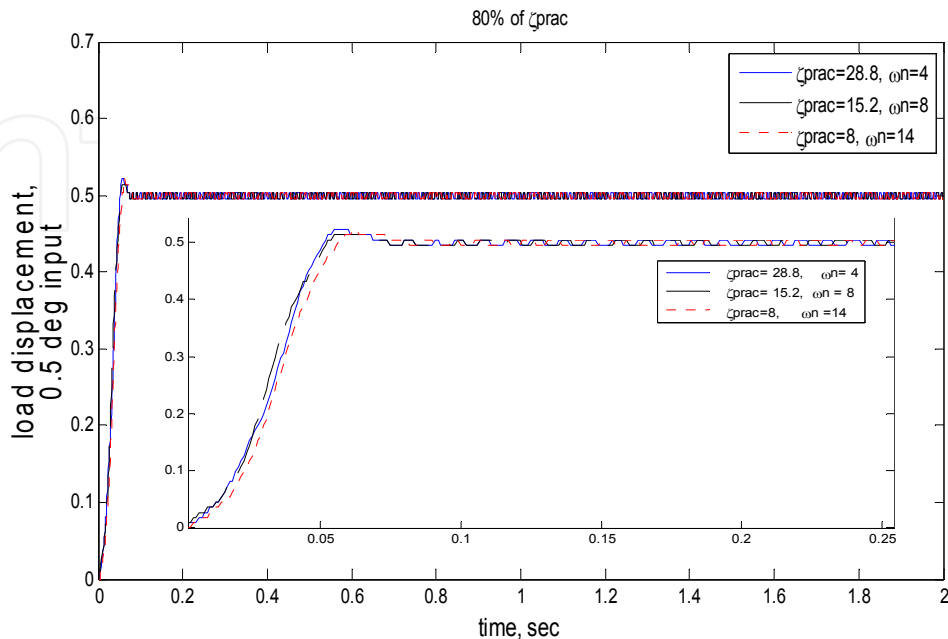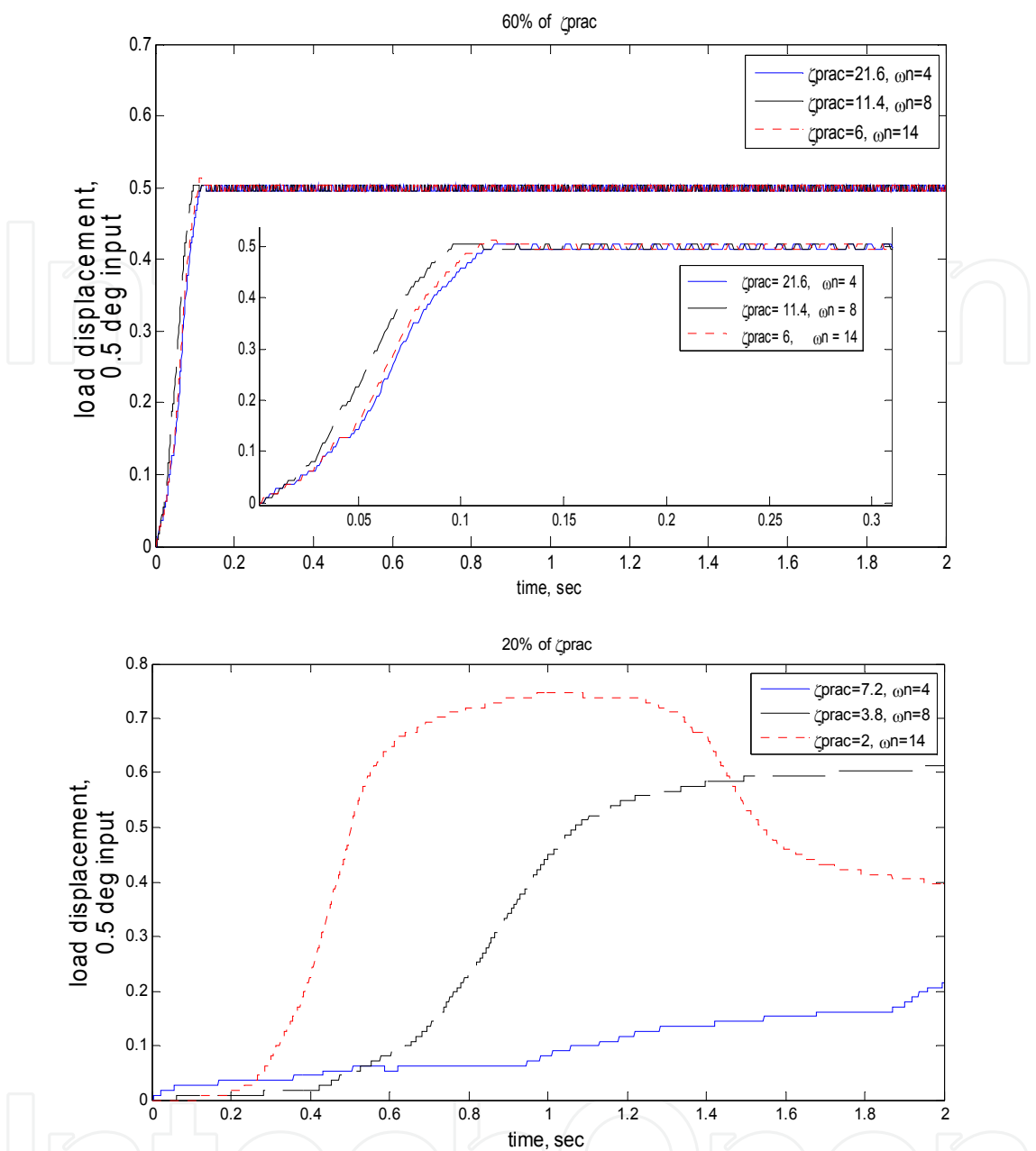
Fig. 8. Response of the compensator due to 0.5 deg step input

while the real component determines the damping level. The larger the magnitude of the real part, the greater the damping (William East & Brian Lantz, 2005).

A NF consists of a pair of complex zeros and a pair of complex poles. The purpose of the complex zeros defined by ω_f and ζ_f is to cancel the resonance poles of the system. The complex poles defined by ω_o and ζ_o, on the other hand, create an additional resonance and to improve the stability, by increasing gain margin of the plant. If the magnitude of the real value of the poles is large enough, it will result in a well-damped response. The ratio between ζ_f and ζ_o will determine how deep the notch in order to eliminate the resonant frequency of the plant. Parameter K_{dc} will be affected in steady state condition when the transfer function of the NF becomes one.

Figure 9(a) shows where the poles and zeros of the system without the controller are located on the s-plane, which gives unstable responses. In Figure 9(b), NF is added to the system, the poles marked *A* are the ones due to the mechanical resonance. These are cancelled by the complex zeros marked by *B*. Although it is assumed that the NF completely cancels the resonance poles, perfect cancellation is not required. As long as the notches zeros are close enough to the original poles, they can adequately reduce their effect, thereby improving system response.
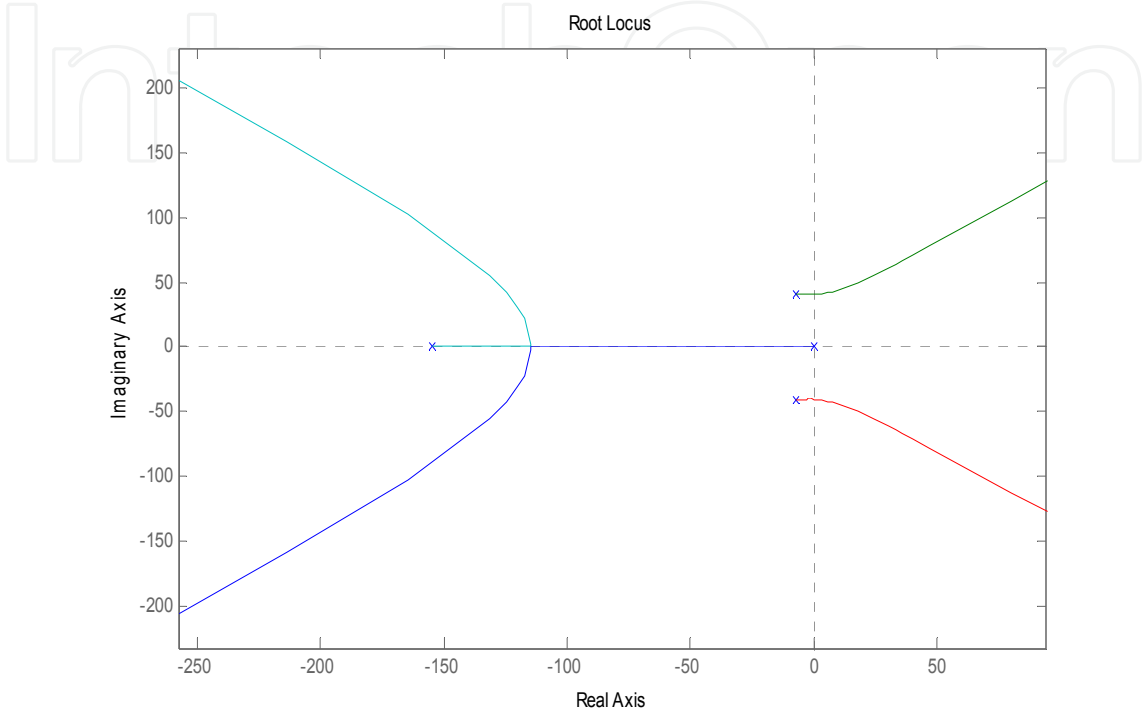
a) Root locus of the system
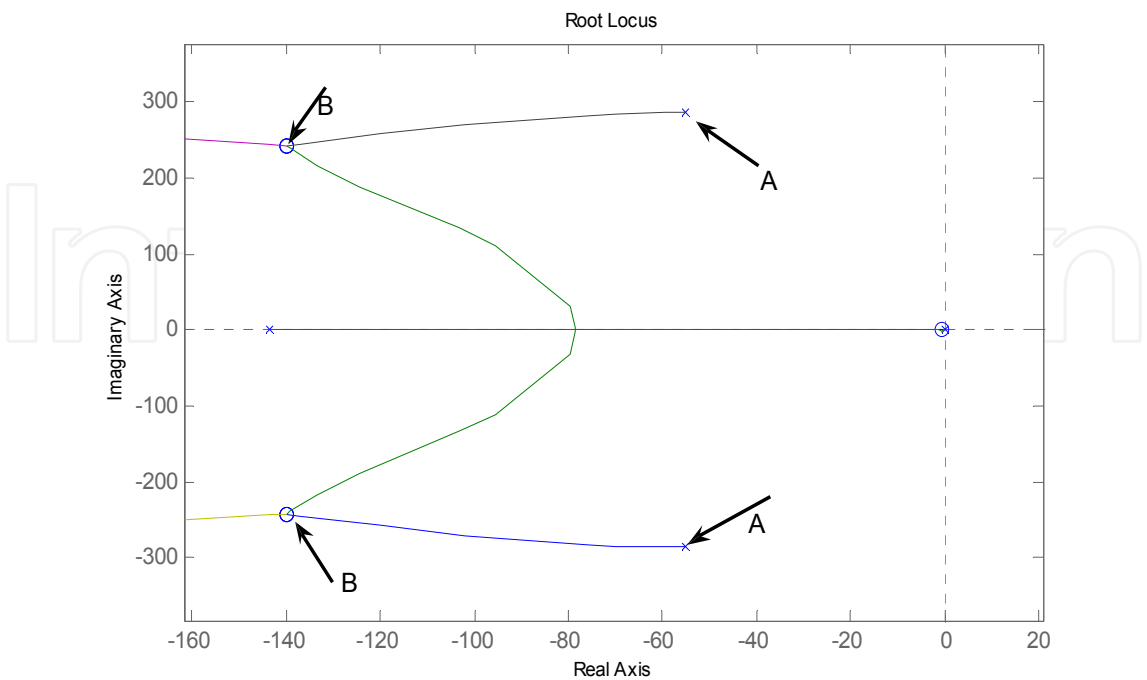
b) Poles and Zeros cancellation of the notch filter
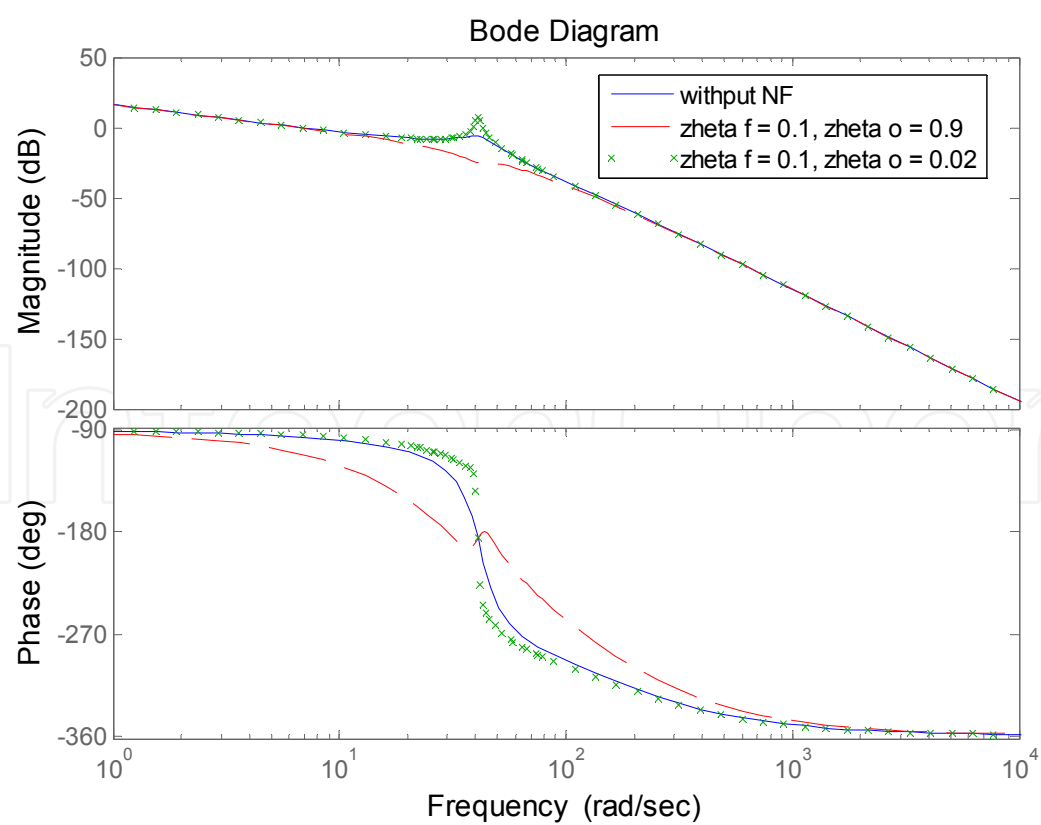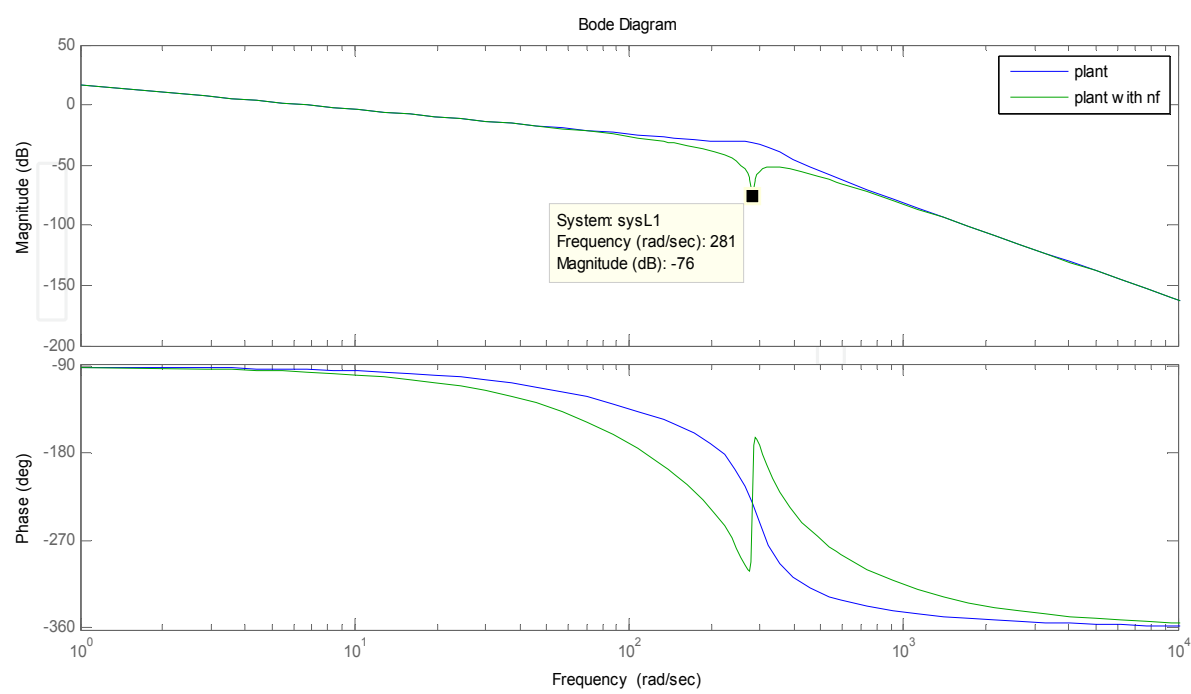
c) Bode diagram of the compensated system with difference ratio of ζ_f and ζ_o
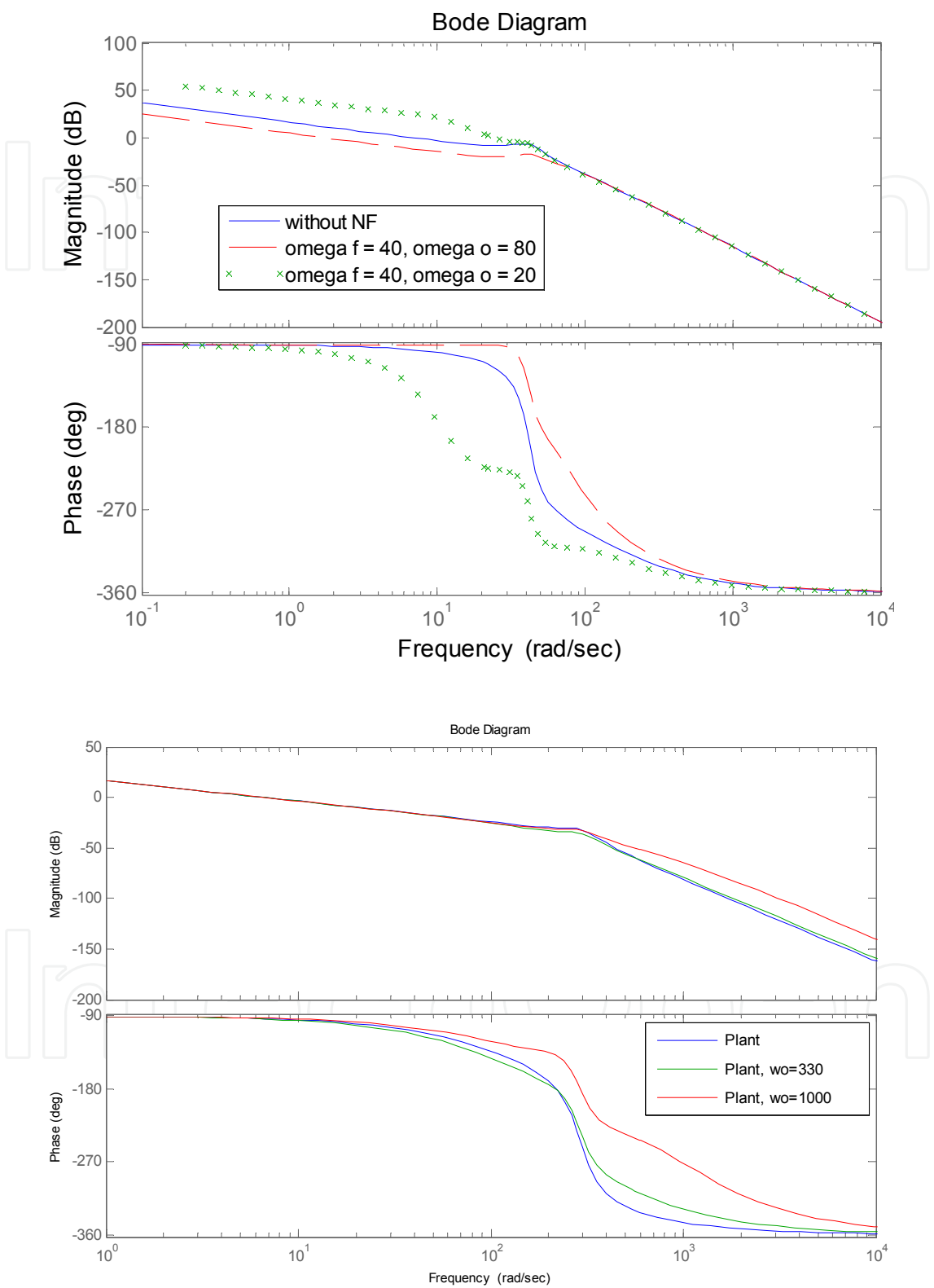
d) Bode diagram of the compensated system with difference ratio of ω_f and ω_o.

Fig. 9. System response

4. Modeling and experimental setup of the systems

Figure 10 shows the simplified diagram of a two-mass rotary positioning system. It consists of mechanical and electromechanical components. The electromechanical (electrical and mechanical) component is the DC motor, which performs the conversion of electrical energy to mechanical energy, and the rest are mechanical components. Two masses, having the moments of inertia, J_m and J_l, are coupled by low stiffness shaft which has the torsion stiffness, K_s and a damping. For the case that the system can be accurately modeled without considering the major nonlinear effects by the speed dependent friction, dead time and time delay, a linear model for two-mass mechanical system can be obtain using the conventional torque balance rule (Robert L.Woods & Kent L.Lawrence, 1997):
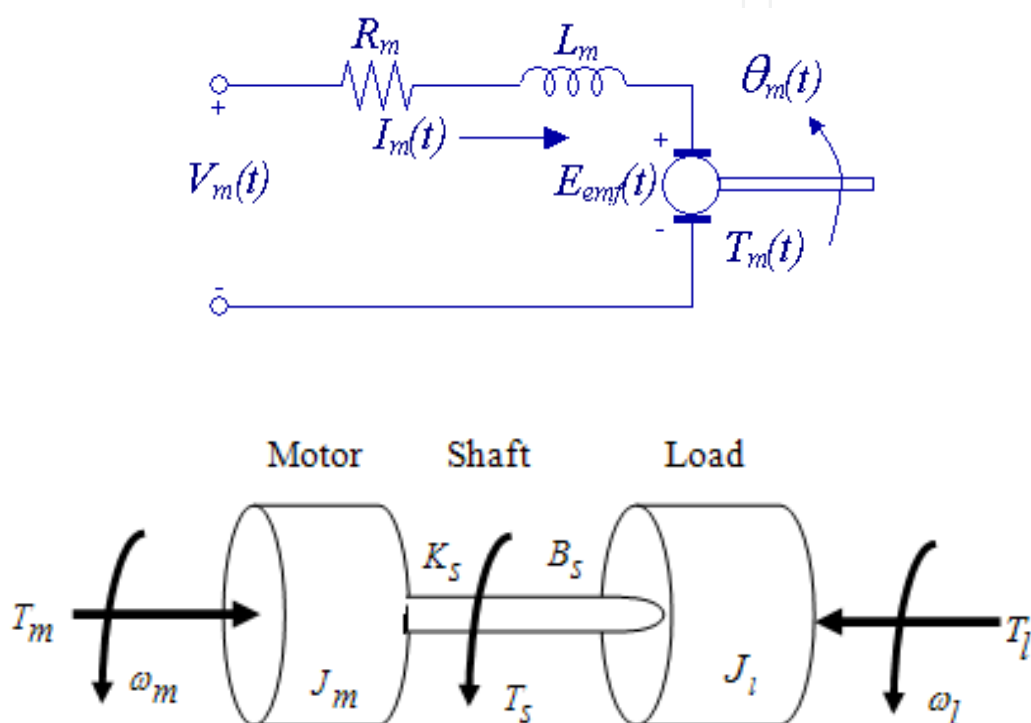

Fig. 10. Schematic diagram of two-mass system

The electrical part of the DC motor is derived by using Kirchoff Voltage Law (KCL),

$$V_m(t) - E_{emf}(t) = L_m \frac{di_m(t)}{dt} + R_m i_m(t) \qquad (22)$$

Next, modeling on the mechanical parts of the system is done by applying Newton's second law of motion to the motor shaft,

$$J_l\left(\frac{d\omega_l}{dt}\right) = T_s - T_l - B_l\omega_l \qquad (23)$$

$$T_s = K_s(\theta_m - \theta_l) + B_s(\omega_m - \omega_l) \qquad (24)$$

with,

$$\frac{d\theta_m}{dt} = \omega_m , \frac{d\theta_l}{dt} = \omega_l \tag{25}$$

where V_m is input voltage, E_{emf} is electromagnetic field, L_m is motor inductance, R_m is motor resistance and i_m is current. J_m and J_l (kgm^2) are the motor and load moments of inertia, w_m and w_l (rad/s) are the motor and load angular speed, T_m and T_l (Nm) are the motor and load disturbance torque, T_s (Nm) is the transmitted shaft torque, B_m and B_l (Nms/rad) are the viscous motor and load frictions, B_s (Nms/rad) is the inner damping coefficient of the shaft and K_s (Nm/rad) is the shaft constant. SI units are applicable for all notations.

The improved NCTF controller is applied to an experimental two-mass rotary positioning systems as shown in Figure 11. It is a two-mass rotary PTP positioning system, which is used in various sequences in industrial applications. It consists of a direct current (DC) motor with encoder, a driver, a low stiffness shaft, load inertia and a rotary encoder. The reading of the encoder is used as a feedback to the controller. The motor is driven by control signals, which are sent to a DC motor driver powered by a power supply. This basic configuration is considered as a normal condition of the system. To measure a load position as a feedback signal of the system, a rotary encoder with 10000 pulses per revolution (ppr) made by Nemicon is used. The object consists of a direct current motor, a driver, inertia load motor, flexible shaft, coupling and inertia load mass.
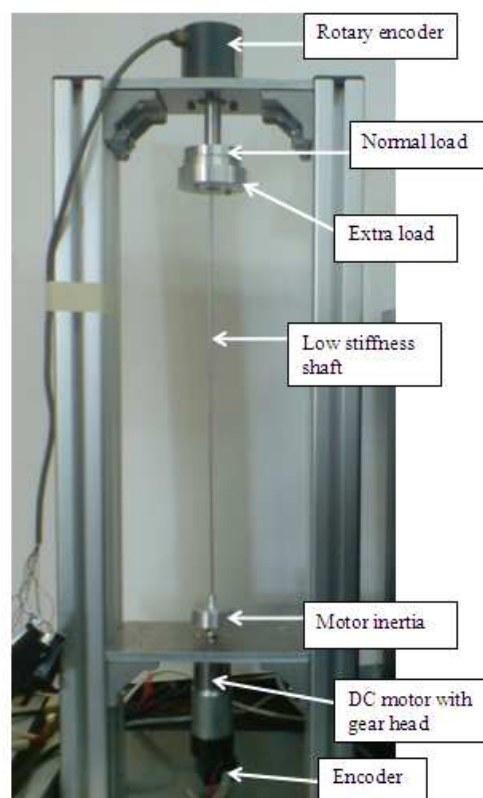

Fig. 11. Experimental two-mass rotary positioning systems

When a load mass has a heavy movable mass, the flexible shaft between the motor mass and load mass work as a spring elements which lead to a vibration. Figure 12 shows step responses to 0.5 deg step input to the experimental rotary system in a normal object condition without the controller. The object will vibrate due to a mechanical resonance and its vibrating frequency is 40 Hz.
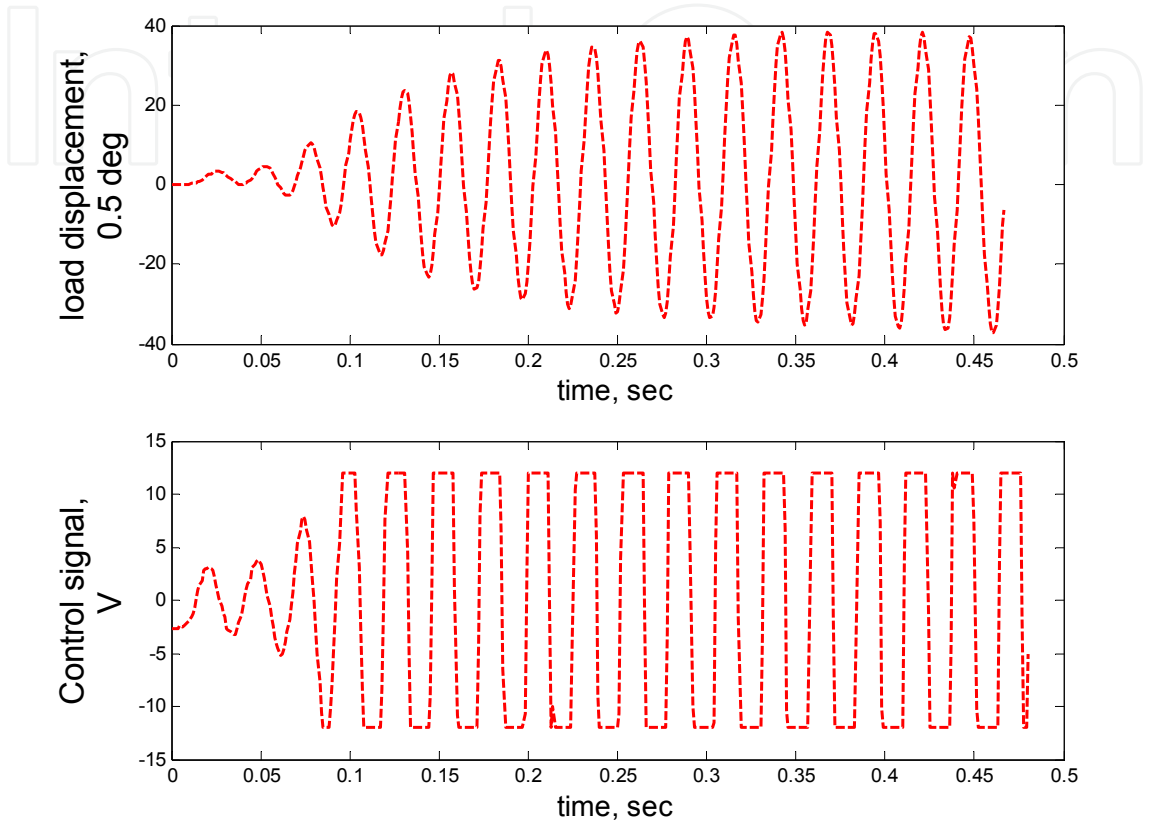

Fig. 12. Vibration responses due to 0.5 deg step response

The detailed block diagram of the model of the object used only for making simulations is shown in Figure 13. In the detailed model of the object, friction and saturation are taken into consideration (De Wit C et al, 1993). The significance of this research lies in the fact that a simple and practical controller can be designed for high precision positioning systems. By improving the NCTF controller, the controller will be more reliable and practical for
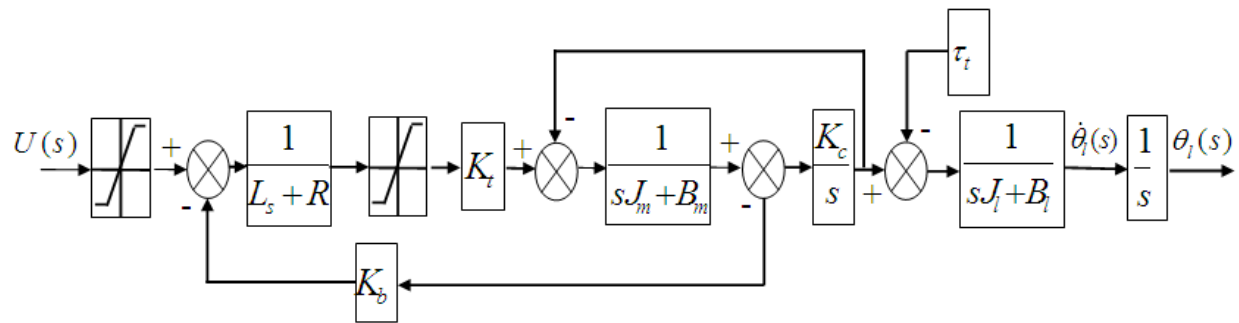

Fig. 13. Dynamic model of the object

realizing high precision positioning systems for two-mass positioning systems compared with conventional PID in term of controller performances. In this section, the continuous time, a linearized mathematical model of the lab scale two-mass rotary system is developed. In order to identify and estimate the parameters, which constitute the two-mass rotary system transfer function, system identification is utilized. Table 1 shows the parameter values of the model for each mechanism.

Parameter	Value	Unit
Motor inertia, J_m	17.16e-6	Kgm^2
Inertia load, J_l	24.17e-6	Kgm^2
Stiffness, K_c	0.039	Nm/rad
Motor resistance, R	5.5	Ω
Motor inductance, L	0.85e-3	H
Torque constant of the motor, K_t	0.041	Nm/A
Motor voltage constant, K_b	0.041	Vs/rad
Frictional torque, τ_t	0.0027	Nm
Motor viscous friction, B_m	8.35e-6	Nms/rad
Load viscous friction, B_l	8.35e-6	Nms/rad

Table 1. Model parameters

5. Experimental results and discussions

Conventional PID controllers were designed based on a Ziegler Nichols (Z-N) and Tyres Luyben (T-L) closed-loop method, using proportional control only. The proportional gain is increased until a sustained oscillation output occur which giving the sustained oscillation, K_u, and the oscillation period, T_u are recorded. The tuning parameter can be found in Table 2 (Astrom K. & Hagglund T, 1995).

Controller	K_p	T_i	T_d
Ziegler Nichlos	$K_u/1.7$	$T_u/2$	$T_u/8$
Tyres Luyben	$K_u/2.2$	T_ux2.2	$T_u/6.3$

Table 2. Controller tuning rule parameters

The significance of this research lies in the fact that a simple and easy controller can be designed for high precision positioning system which is very practical. According to Figure 4, the inclination, m and maximum error rate, h of the NCT are 81.169 and 61.6 respectively. Based on the practical stability limit from Figure 7 and its responses on Figure 8, design parameters for ζ and ω_n are chosen as 9.5 and 10.5 in order to evaluate the performance of NCTF controller. The object will vibrate due to a mechanical resonance and its vibrating frequency is 40 Hz.

From Figure 9, parameters for nominator of NF (ζ_f and ω_f) are selected as 0.7 and 40 Hz while denominator (ζ_o and ω_o) of NF is selected as 0.9 and 100 Hz. Selection of NF parameters are also based on Ruith-Huwirt stability criterion. In order to obtain an always stable continuous closed-loop system, the following constraint needs to be satisfied.

$$2\,\zeta_o\,\omega_o \ge -\,\alpha_2 \qquad\qquad (26)$$

In order to evaluate the effectiveness of improved NCTF controller designed for a two-mass system, the controller is compared with PID controller, which are tuned using Ziegler-Nichols and Tyres-Luyben methods. The PI compensator parameters are calculated from the simplified object parameters (K and a_2) and the design parameters (ω_n and ζ). Table 3 shows the parameters of the compensator of the improved NCTF controller and PID controllers. In order to evaluate the robustness of the improved NCTF control system, the experiments were conducted in two conditions: with normal load and increasing the load inertia as shown in Figure. 14. Normal object is the two-mass experimental rotary positioning with nominal object parameter. Table 4 shows different object parameters for nominal and increased load inertia.
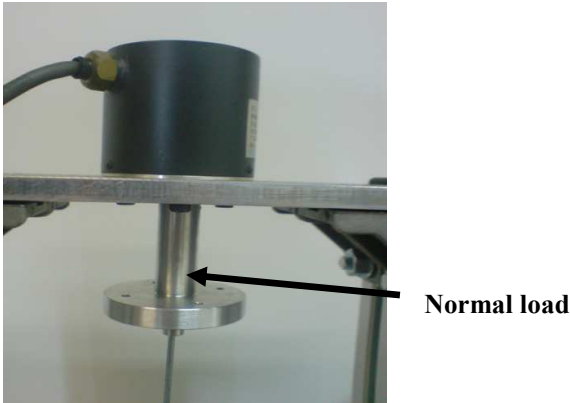
(a)
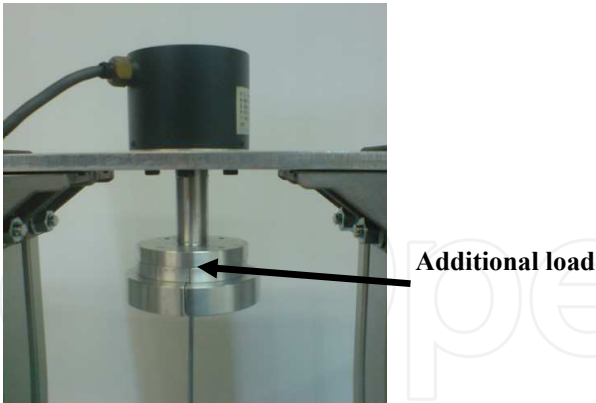
(b)

Fig. 14. Nominal and increased object inertia: (a) Nominal object, (b) Increased object inertia

Controller	K_p	K_i	K_d	ς_f	ω_f	ς_o	ω_o
NCTF	4.79e-1	2.65e-1	-	0.7	40	0.9	60
Z-N PID	78.696	4918.5	0.314	-	-	-	-
T-L PID	59.618	846.85	0.303	-	-	-	-

Table 3. Controller parameters

Object	Inertia
Normal load	$J_l = 14.17 \times 10^{-6}$ kgm^2
Increased inertia load	$2 \times J_l$
	$5 \times J_l$
	$10 \times J_l$

Table 4. Object parameter comparison

Controller			Overshoot (%)	Settling Time (sec)	Ess (deg)
J_l	0.5 deg	Z-N	22.4	0.2	0.108
		T-L	17	0.35	0.108
		NCTF	0	0.083	0.036
	1 deg	Z-N	106.1	0.05	0.072
		T-L	8.9	0.055	0.072
		NCTF	1.7	0.03	0.036
	5 deg	Z-N		unstable	
		T-L		unstable	
		NCTF	6.92	0.043	0.036
$2 \times J_l$	0.5 deg	Z-N	67.47	0.08	0.94
		T-L	18.7	0.25	0.036
		NCTF	0	0.032	0.036
	1 deg	Z-N		unstable	
		T-L	33.2	0.36	0.72
		NCTF	8.9	0.044	0.036
	5 deg	Z-N		unstable	
		T-L		unstable	
		NCTF	11.78	0.052	0.036
$5 \times J_l$	0.5 deg	Z-N	81.8	0.082	0.072
		T-L	13.4	0.25	0.072
		NCTF	0.15	0.072	0.036
	1 deg	Z-N		unstable	
		T-L	39.5	0.3	0.072
		NCTF	47.6	0.09	0.036
	5 deg	Z-N		unstable	
		T-L		unstable	
		NCTF	20.42	0.85	0.036
$10 \times J_l$	0.5 deg Input	Z-N	94.4	0.075	0.072
		T-L	0	0.31	0.072
		NCTF	20.6	0.07	0.036
	1 deg Input	Z-N		unstable	
		T-L	47.6	0.35	0.072
		NCTF	54.8	0.09	0.036
	5 deg input	Z-N		unstable	
		T-L		unstable	
		NCTF	36.44	0.14	0.036

Table 5. Experimental positioning performance comparison

Figure 15 shows the improved NCTF controller for a two-mass rotary positioning system in nominal object and increased object inertia. Figure 16 shows step responses to 0.5, 1 and 5 deg step input when the improved NCTF controller are used to control a nominal object. The positioning performance is evaluated based on percentage overshoot, settling time and positioning accuracy. Figure 17 shows step responses to 0.5, 1 and 5 deg step input to control the increased object with load inertia of twice the nominal object (2 x J_l). Figure 18 and Figure 19 show step responses to 0.5, 1 and 5 deg step input to control the increased object inertia with five and ten times of the nominal object one, i.e 5 x J_l and 10 x J_l. Table 5 presents the experimental positioning performance. An average of 20 similar experiments was conducted.

With nominal object, the improved NCTF controller gives the smallest percentage of overshoot, fastest settling time and a better positioning accuracy than both PID controllers. Unlike the improved NCTF controller for the two-mass rotary system, the PID controllers results in a vibrating response which is 40 Hz. This vibration caused by mechanical resonance of the system. For increased object inertia, the improved NCTF controller demonstrates good positioning accuracy and stable responses. On the other hand, PID based on Ziegler-Nichols rule resulted in unstable response, faster than Tyres-Luyben method for increased object inertia. Therefore, improved NCTF controller is much more robust to inertia variations compared with the two PID controllers. Moreover, for the experimental results, the improved NCTF controller resulted in positioning accuracy near the sensor resolution.
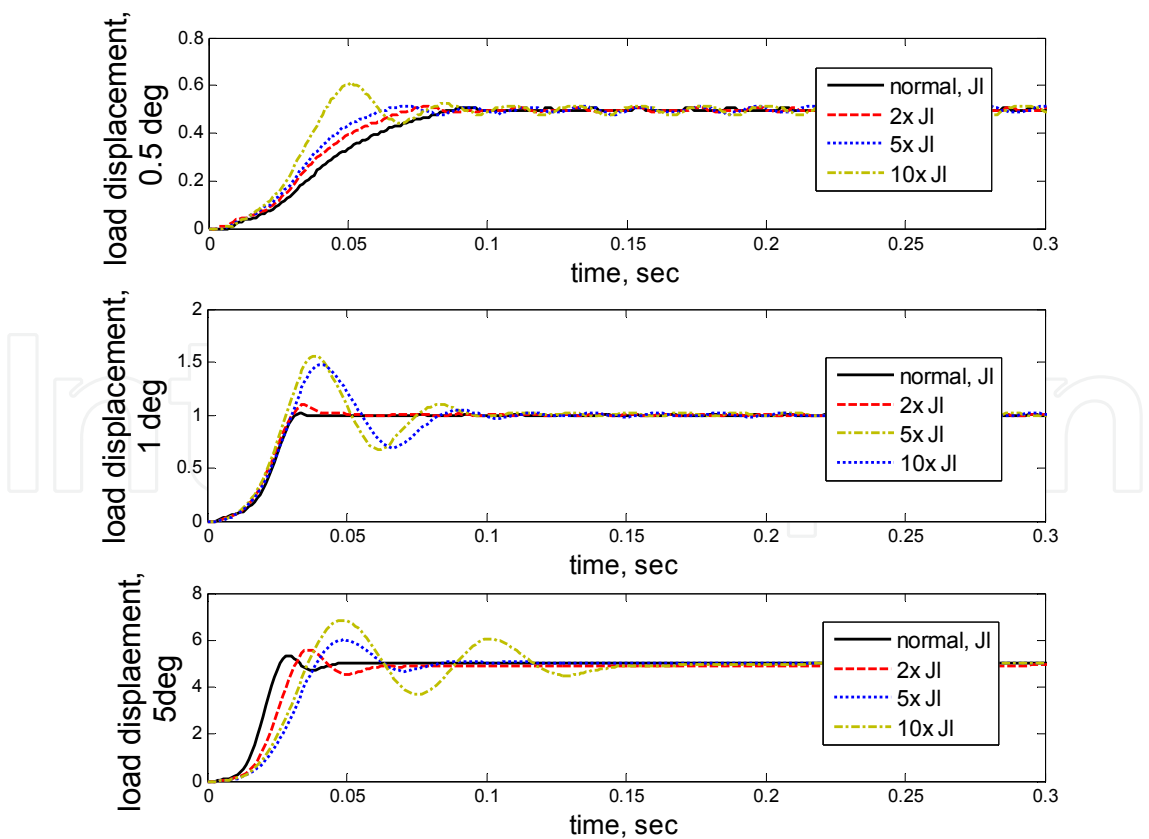

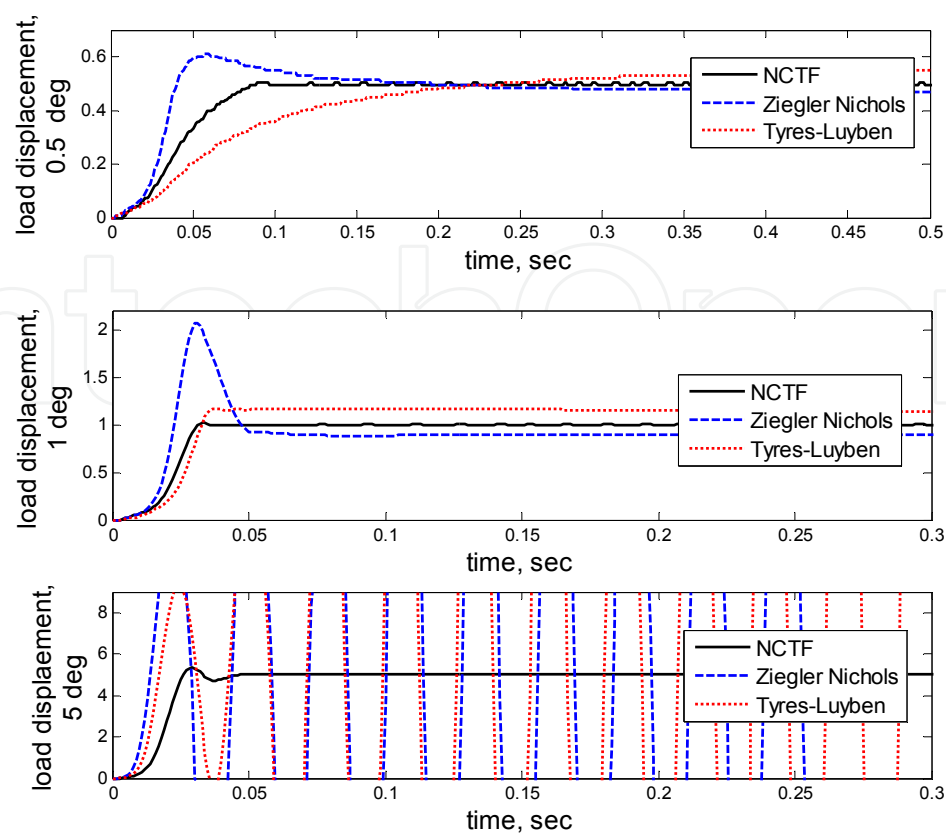Fig. 15. Step response of improved NCTF controller

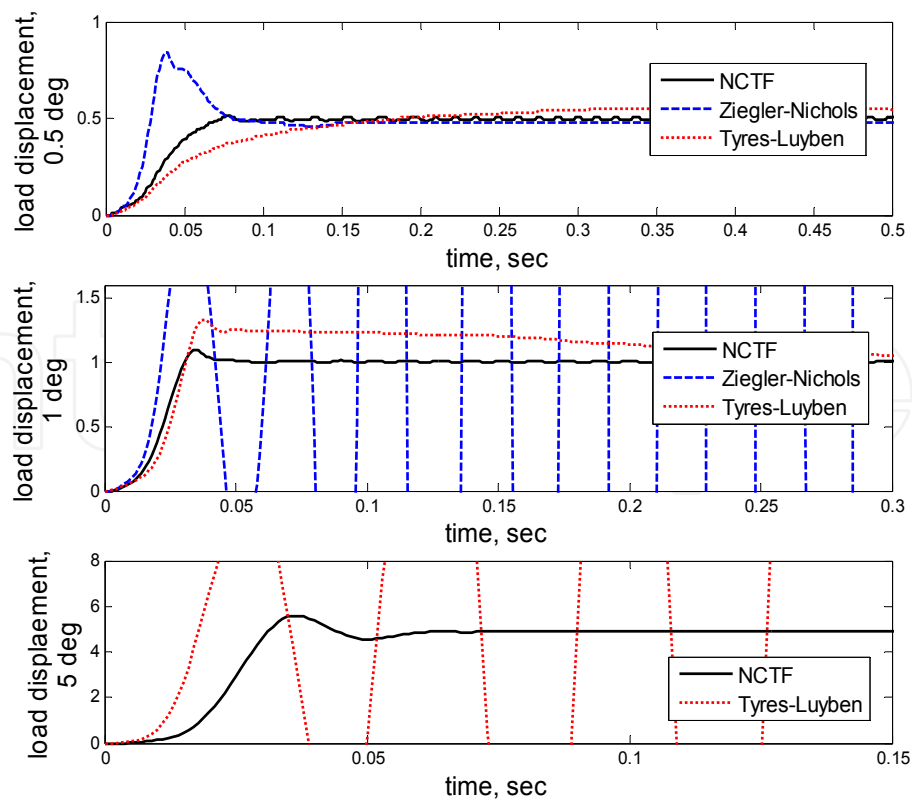Fig. 16. Step response comparison, nominal object condition

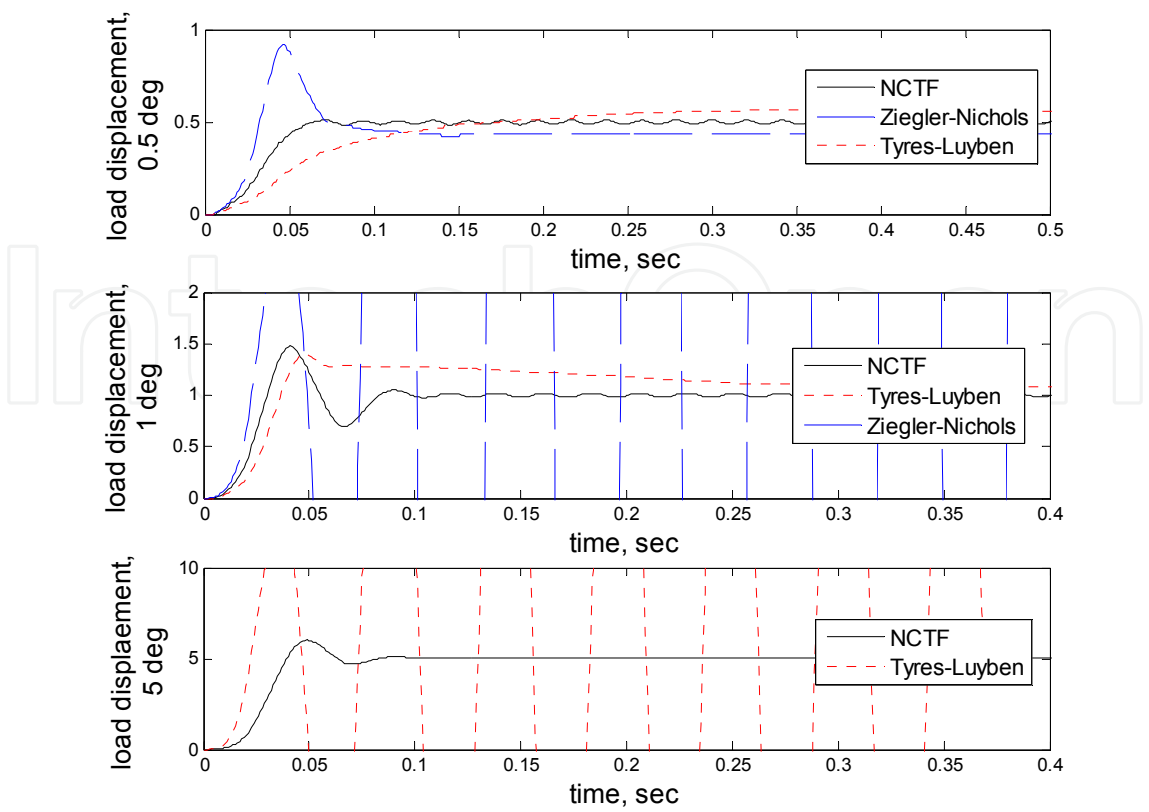Fig. 17. Step response comparison, increased object inertia (2 x J$_l$)

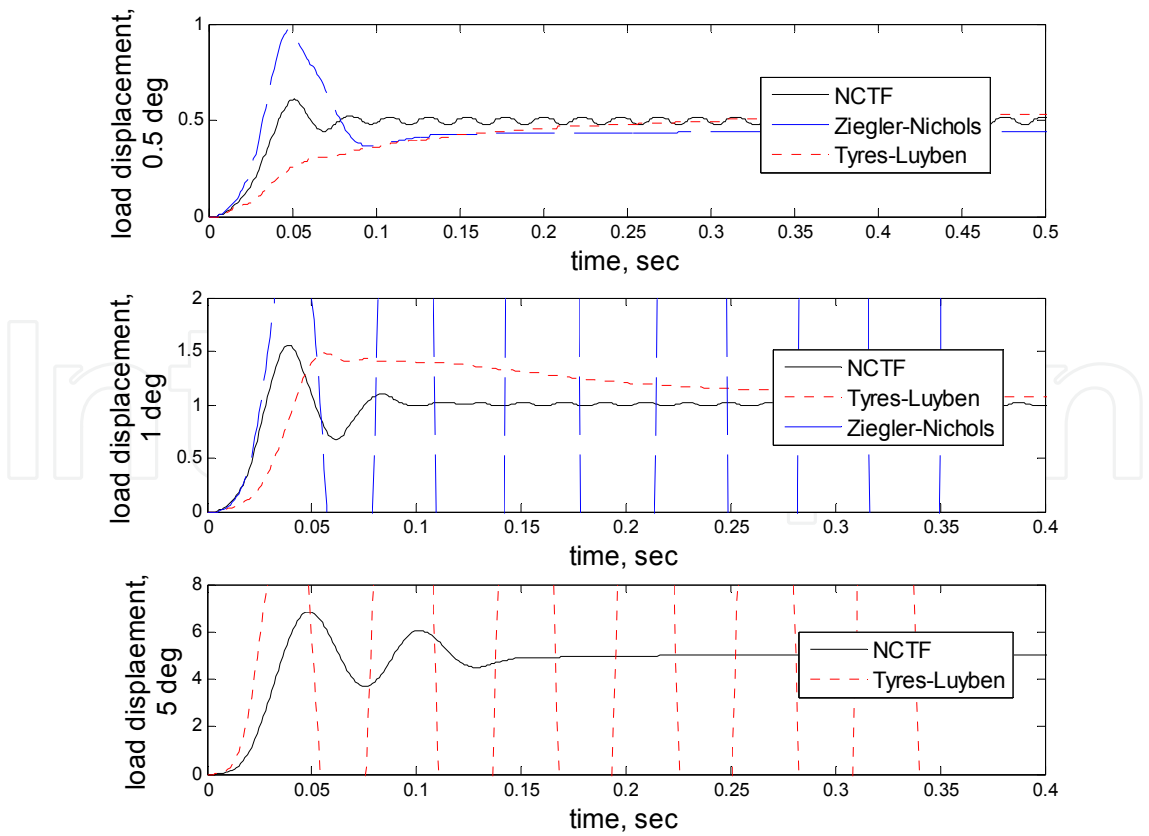Fig. 18. Step response comparison, increased object inertia (5 x J_l)

Fig. 19. Step response comparison, increased object inertia (10 x J_l)

6. Conclusion

This paper has discussed and described the improved practical design of the NCTF controller for two-mass rotary positioning systems. First, the NCT determination was discussed. In order to eliminate the influence of the vibration on the NCT, the vibrating responses are averaged using simple moving averaged filter. Then, the PI with NF compensator is designed based on the NCT information and the object responses. The PI is adopted for its simplicity to force the object motion to reach the NCT as fast as possible and control the object motion to follow the NCT and stop at the origin. The NF is adopted to eliminate the vibration frequency caused by mechanical resonance of the system.

Through experiments using two-mass rotary experimental positioning systems, the effectiveness and robustness of the improved NCTF controller was evaluated. The experimental results confirmed that the improved NCTF controller for a two-mass system has better performance in term of percentage of overshoot, settling time and positioning accuracy than PID controllers. The improved NCTF controller for two-mass system resulted in an insignificant vibration. Moreover, experimental resulted prove that the improved NCTF controller was much more robust to inertia variations than PID controllers designed based on Ziegler-Nichols and Tyres-Luyben methods. Therefore, the improved NCTF controller for two-mass rotary positioning systems that includes the NF will have a better performance than the PID controllers with NF. Applications of the NCTF concept to multi-mass positioning systems can be done for further study.

7. Acknowledgment

8. References

Armstrong-Helouvry B., Dupont P, and De Wit C. (1994). A survey of models, analysis tools and compensation method for the control of machines with friction. *Automatica*, Vol. 30, No. 7, pp. 1083-1138.

Astrom K. & Hagglund T, PID controllers: Theory, design and tuning. *Instrument Society of America*, 1995.

Crowder R.M. (1998). *Electric drives and theier controls*, Oxford: Oxford University Press

De Wit C., Olsson H., Astrom K.J & Lischinssky, Dynamic friction models and control design, *Proceedings American Control Conference,* San Francisco, USA, 1993, pp. 1920-1926.

Dorf, R.C., & Bishop, R.H. (2008). *Modern Control System*. Pearson Prentice Hall.

Guilherme Jorge Maeda & Kaiji Sato, Practical control method for ultra-precision positioning using a ballscrew mechanism. *Precision Engineering Journal,* Vol. 32(2008)309-318, November 2007.

Mohd Fitri Mohd Yakub, Wahyudi Martono and Rini Akmeliawati, "Performance Evaluation of Improved Practical Control Method for Two-Mass PTP Positioning Systems", *Proceedings of the 2010 IEEE Symposium on Industrial Electronics & Applications (ISIEA2010)* 3–5 October 2010, Penang, pp. 550-555.

Oppenheim A.V. & Schafer R.W, Discrete Time Signal Processing. *Englewood Cliffs*, Prentice Hall, 1999.

Robert L.Woods and Kent L.Lawrence, Modelling and Simulation of Dynamic Systems, Prentice Hall Inc, 1997.

Slotine, J. J. & Li, W. P. (1991). Applied Nonlinear Control, Prentice-Hall, Inc., New Jersey

Townsend WT and Kenneth Salisbury J, The effect of coulomb friction and stiction on force control, *IEEE Int Conf Robot Automat* 1987;4:883-9.

Wahyudi. (2002). *New practical control of PTP positioning systems*. Ph.D. Thesis. Tokyo Institute of Technology.

Wahyudi, Sato, K., & Shimokohbe, A. (2003) Characteristics of practical control for point-to-point positioning systems: effect of design parameters and actuator saturation. *Precision Engineering*, 27(2), 157-169.

William East & Brian Lantz, Notch Filter Design, August 29, 2005.

Yonezawa H., Hirata H. and Sasai H. (1990). Positioning table with high accuracy and speed. *Annal CIRP*. Vol. 39, pp. 433-436.

PID Controller Design Approaches - Theory, Tuning and Application to Frontier Areas

Edited by Dr. Marialena Vagia

ISBN 978-953-51-0405-6

Hard cover, 286 pages

Publisher InTech

Published online 28, March, 2012

Published in print edition March, 2012

First placed on the market in 1939, the design of PID controllers remains a challenging area that requires new approaches to solving PID tuning problems while capturing the effects of noise and process variations. The augmented complexity of modern applications concerning areas like automotive applications, microsystems technology, pneumatic mechanisms, dc motors, industry processes, require controllers that incorporate into their design important characteristics of the systems. These characteristics include but are not limited to: model uncertainties, system's nonlinearities, time delays, disturbance rejection requirements and performance criteria. The scope of this book is to propose different PID controllers designs for numerous modern technology applications in order to cover the needs of an audience including researchers, scholars and professionals who are interested in advances in PID controllers and related topics.

INTECH
open science | open minds